ACS Combinatorial Science

Research Article

pubs.acs.org/acscombsci

Modeling Preparation Condition and Composition–Activity Relationship of Perovskite-Type $La_xSr_{1-x}Fe_yCo_{1-y}O_3$ Nano Catalyst

Samira Arefi Oskoui,[†] Aligholi Niaei,*[,†] Hui-Hsin Tseng,[‡,§] Dariush Salari,[†] Behrang Izadkhah,[†] and Seyed Ali Hosseini[∥]

[†]Department of Applied Chemistry and Chemical Engineering, Faculty of Chemistry, University of Tabriz, Tabriz, Iran

[‡]School of Occupational Safety and Health, Chung Shan Medical University, Taichung 402, Taiwan, Republic of China

[§]Department of Occupational Medicine, Chung Shan Medical University Hospital, Taichung 402, Taiwan, Republic of China

[∥]Department of Chemistry, Faculty of Science, Urmia University, 57159, Urmia, Iran

Supporting Information

ABSTRACT: In this paper, an artificial neural network (ANN) is first applied to perovskite catalyst design. A series of perovskite-type oxides with the $La_xSr_{1-x}Fe_yCo_{1-y}O_3$ general formula were prepared with a sol–gel autocombustion method under different preparation conditions. A three-layer perceptron neural network was used for modeling and optimization of the catalytic combustion of toluene. A high R^2 value was obtained for training and test sets of data: 0.99 and 0.976, respectively. Due to the presence of full active catalysts, there was no necessity to use an optimizer algorithm. The optimum catalysts were $La_{0.9}Sr_{0.1}Fe_{0.5}Co_{0.5}O_3$ (T_c = 700 and 800 °C and [citric acid/nitrate] = 0.750), $La_{0.9}Sr_{0.1}Fe_{0.82}Co_{0.18}O_3$ (T_c = 700 °C, [citric acid/nitrate] = 0.750), and $La_{0.8}Sr_{0.2}Fe_{0.66}Co_{0.34}O_3$ (T_c = 650 °C, [citric acid/nitrate] = 0.525) exhibiting 100% conversion for toluene. More evaluation of the obtained model revealed the relative importance and criticality of preparation parameters of optimum catalysts. The structure, morphology, reducibility, and specific surface area of catalysts were investigated with XRD, SEM, TPR, and BET, respectively.

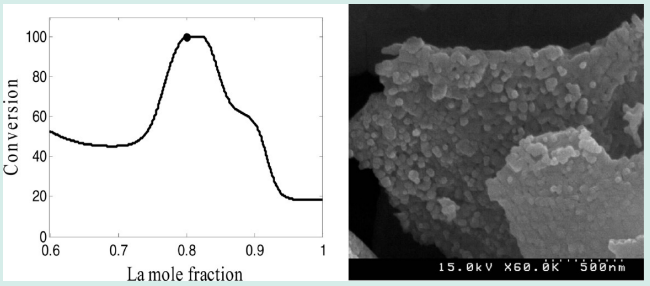

KEYWORDS: *perovskite, $La_xSr_{1-x}Fe_yCo_{1-y}O_3$, sol–gel, catalytic oxidation, toluene, catalyst design, ANN modeling*

1. INTRODUCTION

According to test method D3960 of the American Society for Testing and Materials, VOCs are organic compounds having a vapor pressure larger than 13.3 Pa at 25 °C.[1] Volatile organic compounds (VOCs) are an issue of major concern for many scientists worldwide because of their contribution to major environmental problems such as stratospheric ozone depletion, photochemical smog formation, global warming, and an odor nuisance.[2] In addition, both VOCs and their degradation products may be important in the epidemiology of respiratory disorders and cancer.[3] Toluene is a common VOC used as raw material in manufacturing many organic compounds and also used as a solvent in several industries. This compound has a toxic nature and causes mild macrocytic anemia in people working with it.[4] Catalytic oxidation is one of the effective and economic techniques for the treatment of a low concentration VOC stream. Metal oxide catalysts are alternatives for noble catalysts. Among the metal oxides, perovskite-type mixed oxides due to their high catalytic activity in the oxidation of VOCs and thermal stability in the high temperature range of operation are of importance. These materials are represented by the ABO_3 general formula, where A is lanthanide and/or alkaline earth metal ion and B is a transition metal ion. Both A and B cations can be partially substituted, leading to multicomponent oxides ($A_{1-x}A'_xB_{1-y}B'_yO_3$).[5,6] Partial substitution of the A site causes lattice defects and abnormal valences in B site cations that usually enhance catalytic activity. The B-site partial substitution brings about synergistic effects and influences the stability of the crystalline structure.[5]

Catalyst design is a tedious and a complex process involving many steps, many variables, and complex interactions among these variables that make the experimental studies quite expensive and time-consuming.[7] It is possible to obtain an efficient catalyst for a chemical reaction by catalyst design.[8] In catalyst design, components of the catalyst and synthesis conditions are selected through a systematic method by using the available knowledge and concepts of catalysis.[9] Two different methods can be recognized for catalyst design: the traditional method and the computer-aided-design catalyst (CADC) method. In the traditional method, the main components of the catalyst are selected by considering the reaction mechanism, and subsequently the best catalyst is determined from several experiments. So a lot of money, manpower, time, and material resources are necessary to obtain

Received: February 2, 2013
Revised: August 19, 2013
Published: October 8, 2013

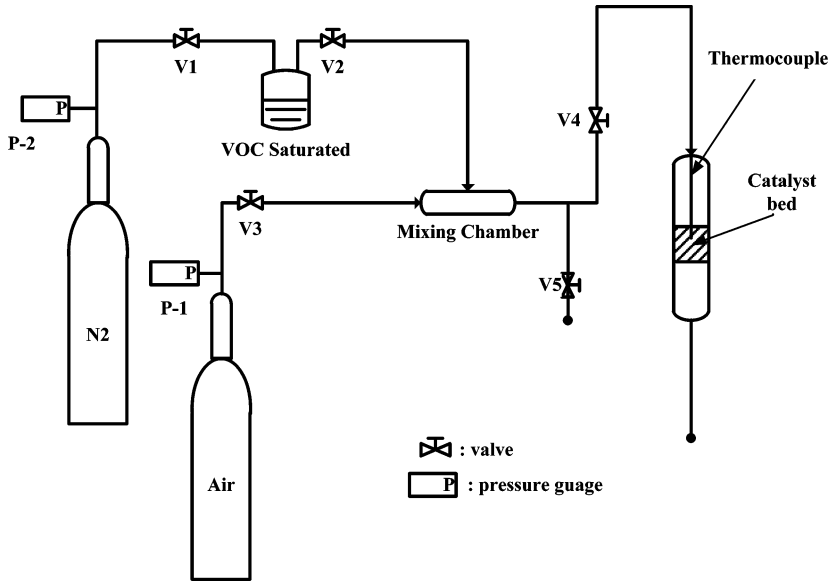

Figure 1. Schematic of the setup for catalytic oxidation of VOCs.

a suitable catalyst with the traditional method. In addition, it is impossible to design some highly efficient catalysts for a new reaction in a short time through traditional catalyst design methods. According to the rapid development of computer science, chemists found the chance to use the CADC method for catalyst design. In comparison with the traditional method, the CADC method does not need to know the catalytic mechanism completely and could design better catalysts in a short time with fewer experiments. In the past 20 years, computer-aided catalyst design with ANN has been reported to design catalysts for different processes by some researchers. Artificial neural networks (ANNs) are computing systems that are based on the concepts of neurons in biology.[10] Hou et al.[11] in 1997 used ANN for designing a catalyst for propane ammoxidation. Huang et al.[12] in 2001 developed an improved back-propagation network to simulate the relations between components of the catalyst and aspects of catalytic performance, which include C_2 selectivity and conversion of methane. Serra et al.[13] in 2003 used ANNs for modeling the kinetics of catalytic hydroisomerization of different *n*-paraffins. They proposed a novel methodology for modeling catalytic data employing already-trained neural networks by using experimental results from the catalytic reactions. Baumes et al.[14] in 2004 used ANNs to predict performances of catalysts for the water gas shift reaction. This search showed that ANNs used as a classifier tool within the course of an evolutionary strategy are high performing and well suited for high throughput heterogeneous catalysis. Izadkhah et al.[15] in 2012 coupled a neural network model with a genetic algorithm to design and optimize bimetallic ZSM5 supported catalysts for catalytic oxidation of volatile organic compounds. Niaei et al.[16] in 2012 designed a modified H-ZSM-5 catalyst for catalytic conversion of methanol to gasoline range hydrocarbons (MTG) by using the neuro-genetic approach. The aim of this work is modeling and optimization of preparation conditions of the catalyst. In the present study, the nanostructured $La_xSr_{1-x}Fe_yCo_{1-y}O_3$ perovskite mixed oxides, prepared with the sol–gel combustion method, were used as novel catalysts for catalytic oxidation of toluene. The structure, morphology, reducibility, and specific surface area of catalysts were investigated with XRD, SEM, TPR, and BET, respectively. According to the complex interaction among catalyst components and absence of a clear reaction mechanism for toluene combustion over perovskite, artificial neural networks were used for modeling the relationship between composition and catalyst activity. To minimize the repetitious trial-and-error process and for implementation of experiments in a random manner, CCD (Central Composite Design) as an experimental design method with four factors (La mole fraction, Fe mole fraction, calcinations temperature (Tc), and molar ratio of citric acid to the total metal nitrates) was used. All catalysts based on experimental design array were prepared and tested in three different temperatures (220, 260, and 300 °C), so the required database for ANN modeling was produced. A three-layer perceptron neural network was used to model the relationship between catalytic performances and catalyst design parameters. The obtained ANN model was used to determine the relative importance of design parameters. Optimum catalysts (catalysts with full activity) were selected, and more investigation was done on them. The present paper is the first report applying ANN for modeling the composition–activity relationship in perovskite catalysts for the toluene combustion process.

2. EXPERIMENTAL PROCEDURES

2.1. Synthesis of Catalyst. The perovskite-type oxides were prepared by sol–gel auto combustion. Analytical grade $La(NO_3)_3{\cdot}6H_2O$, $Sr(NO_3)_2$, $Fe(NO_3)_3{\cdot}9H_2O$, $Co(NO_3)_2$, and citric acid ($C_6H_8O_7{\cdot}H_2O$) (Merck) were used as raw materials. Stoichiometric amounts of mentioned metal nitrates, based on experimental design array, were dissolved together in a minimum amount of distilled water to get a clear solution (Sol). The solution was heated on a hot plate; when the temperature of the solution was raised to 70 °C, an appropriate amount of citric acid monohydrate was added to the solution. The molar ratio of citric acid to the total nitrates in the solution mixture was kept at the quantity that the experimental design proposed. The solution was stirred vigorously and heated at 80 °C for dehydration. During the dehydration process, a polycondensation reaction happened between citric acid and nitrates. At last, a sticky gel was obtained and burned by heating

dx.doi.org/10.1021/co400017r | ACS Comb. Sci. 2013, 15, 609–621

at 200 °C on a hot plate and turned into a dark powder. The powder was calcined in two steps. First, powder was calcined at 600 °C for 1 h, and then it was calcined under a temperature proposed by experimental design for 4 h.

2.2. Catalyst Characterization. X-ray diffraction (XRD) studies were carried out on a Siemens D500 diffractometer working with a K_α line of copper (λ = 0.154 nm) at a scan rate of 4° min^{-1}. Measurements of the samples were carried out in the 2θ range of 15−67°. The mean crystal sizes were estimated using the Scherer equation, $D = K\lambda/\beta \cos\theta$, where K = 0.89, λ =0.15418 nm, β is the half peak width of the X-ray reflection, and θ is the diffraction angle.

For temperature-programmed reduction (TPR) experiments, a chembet-3000 apparatus was used. The H_2-TPR was carried out under a 10 mL min^{-1} flow of 5% H_2 in Ar, heating 10 °C min^{-1} up to 1000 °C.

Furthermore, the shape and size of the synthesized particles were determined via scanning electron microscopy (SEM) with a Hitachi s-4200 instrument with precoating samples with gold.

Specific surface areas were determined on a chembet-2400 apparatus with nitrogen as the adsorbate by a single point BET method.

2.3. Evaluation of Catalytic Performance. The schematic view of the setup used for catalytic study of VOC combustion is shown in Figure 1. Catalytic oxidation reactions were carried out in a conventional fixed bed reactor under atmospheric pressure and at different temperatures (220, 260, and 300 °C). The total flow rate through the reactor was set at 100 cm^3 min^{-1}. The VOC-laden air stream at a fixed concentration as feed to the reactor was generated by bubbling the nitrogen gas at a suitable flow rate through the VOC saturators. The catalytic activity tests and the preparation of aged catalyst samples were performed in a 0.008-m-inner-diameter and 0.6-m-long cylindrical quartz reactor heated with an electrical furnace. The gas hourly space velocity (GHSV) was measured under inlet conditions of about 6000 h^{-1}. The catalytic reactions were performed under steady state conditions in which all process variables remained constant with time at any given point in the reactor before any measurement was made. The feed and product gases were analyzed using a Shimadzu 2010 gas chromatograph (GC) equipped with a FID detector and a CBP1 column of shimadzu columns (l = 25 m, i.d. = 0.25 mm).

3. MODELING DETAIL

3.1. Design of Experiment Using Central Composite Design. To reduce the number of experiments and to arrange the experiments with various combinations of independent variables, a central composite design (CCD) was employed to design the experiments. The effect of the following four factors (independent variables) on the conversion of toluene (response) was studied: the mole fraction of La, the mole fraction of Fe, calcination temperature (°C), and molar ratio of citric acid to the total nitrates in the solution mixture. The ranges of the independent variables were determined by considering the literature.[17,18] The ranges and levels used in the experiments are given in Table 1.

The experimental design matrix resulted from the CCD consists of 31 sets of coded conditions expressed in natural values. Experiments include seven replications at the center point, eight axial points, and 16 factorial points.

3.2. Neural Networks. The artificial neural networks used in this work were created by writing computer codes in

Table 1. Independent Variables and Their Levels in the Experimental Design

	levels				
independent variables	−2	−1	0	1	2
mole fraction of lanthanum	0.6	0.7	0.8	0.9	1
mole fraction of iron	0.34	0.5	0.66	0.82	0.98
calcination temperature (°C)	650	700	750	800	850
[citric acid]/[total nitrate]	0.075	0.3	0.525	0.750	0.975

MATLAB 7.2 software. For modeling the catalyst performance, a multilayer perceptron (MLP) was developed. The MLP neural networks are the most common networks of the feed forward kind, so signal transmission between neurons is only possible from a lower layer to a higher layer. According to the literature, these networks have been used to estimate relationships between catalytic performance and chemical composition, physical properties, and reaction conditions.[19−21]

The MLP neural networks consist of a number of layers of neurons including an input layer, an output layer, and one or more hidden layers between the input and output layers.[22] The number of neurons in the input and output layers corresponds to the number of independent variables and the number of dependent variables (responses), respectively. In this study, the input layer contained five neurons including mole fraction of La, mole fraction of Fe, calcination temperature (°C), and molar ratio of citric acid to total nitrates in the solution mixture as catalyst preparation variables and the reaction temperature (T_R) as an operational variable. There was one output neuron in the output layer that was the conversion of toluene, which represented the activity of the catalyst. Indeed, there is no general guideline to determine the appropriate number of hidden layers and their neurons; however, theoretically the MLP with one hidden layer is enough to solve any problem that MLP with two hidden layers can solve.[23] Therefore, a MLP with one hidden layer was used for model development. The optimum number of neurons should be used in a hidden layer in order to reach the model which simulates experimental results best. It is well-known that a network with few numbers of neurons cannot model the relationship between the input and the output parameters. On the other hand, a network with too many neurons may cause overfitting. To determine the optimum number of hidden layer neurons, training of the model started with a small number of neurons and then continued by adding neurons to the hidden layer until the best model without overfitting was obtained. All attempts were repeated five times with the results being stated as an average of five turns. The standard deviation of error value was used to evaluate and compare the statistical fitness of various neural networks.

The tan-sigmoid (hyperbolic tangent sigmoid) was used as the activation function of the hidden layer, because it is a good choice for many nonlinear functions (eq 1). The activation function used for the output layer was a linear function (eq 2).

$$f(x) = \frac{1}{1 + \exp(-x)} \quad (1)$$

$$f(x) = x \quad (2)$$

dx.doi.org/10.1021/co400017r | ACS Comb. Sci. 2013, 15, 609−621

Standard back-propagation (BP) is the most popular training algorithm for minimizing the error function for an MLP neural network, and there are several different BP training algorithms. In this study, the gradient descend algorithm (traingdm) was used for training as a neuron weights optimizer.

It should be noted that before training, input data were normalized into the range of −1 to +1 according to eq 3, but target values were used without normalizing.

$$x_i = \frac{2X_i}{X_{\max} - X_{\min}} - 1 \tag{3}$$

where X_i is the natural value of the ith variable, x_i is the dimensionless coded value of the ith variable, and $X_{\max}$ and $X_{\min}$ are the highest and the lowest limits of the ith variable, respectively.

Relative importance of the input parameters (catalyst preparation and operational variables), which indicates the effect of each input parameter on the output factor (toluene conversion), was calculated using eq 4.[24]

$$S_s = \frac{\sum_j^n (w_{sj}u_{jk}/\sum_i^m w_{ij})}{\sum_i^m \sum_j^n (w_{ij}u_{jk}/\sum_i^m w_{ij})} \tag{4}$$

S_s shows the relative significance of the sth parameter. w_{ij} is the weight that connects the ith input point to the jth neuron of the hidden layer. u_{jk} is the weight that connects the jth hidden layer neuron to the kth output neuron. m is the number of input neurons. n is the number of neurons of the hidden layer, and k is the number of outputs.

Optimum catalysts which showed full activity in toluene combustion were selected and underwent more deliberation. The impact of each preparation parameter on optimum catalyst performance was investigated, and also, the critical value of preparation parameters was determined.

4. RESULTS AND DISCUSSION

4.1. Toluene Conversion Modeling. At first, a linear model and Response Surface Area (RSM) as a DoE method were used for modeling the relationship between catalyst preparation parameters and activity in perovskite catalysts. Low R^2 values (Table 2) for both the linear model and obtained model of RSM indicates the inability of the mentioned models to model the parameter space of perovskite catalyst synthesis. This conclusion can be verified by studying the ANN model, which shows modeled parameter space is very complicated and has various volcano type behaviors in almost the whole of parameter space. So the only way to model such a complicated parameter space is intelligent methods such as ANN, which is able to model the complicated parameter spaces. Indeed utilization of ANN to model simple parameter spaces is meaningless because it makes the problem more complicated. On the other hand, utilization of linear model or classical DoE for modeling of complicated parameter spaces is not reasonable because it cannot model the complicated parameter spaces with acceptable error. Therefore, perovskite catalyst synthesis parameter space, as a very complicated parameter space, cannot be modeled using simple methods such as linear model, classical DoE and so forth and should be modeled using more effective methods such as ANN.

Table 2. R^2 Values for the Linear Model and Model Obtained from RSM

model	R^2
linear model	5%
RSM (220 °C)	51.4%
RSM (260 °C)	60.5%
RSM (300 °C)	57.8%

The experimental toluene conversion at various temperatures on the CCD proposed catalysts was used as a database for the neural network model (Supporting Information). It should be noticed that the average of toluene conversion in repeated central points was used for modeling. This database involves 75 patterns, and each pattern consisted of six features (four features for preparation conditions, one feature for reaction temperature, and one feature for conversion of toluene as output).

Two main steps can be recognized in the ANN model development: determination of optimum topology and validation of the model. For modeling, the data are randomly divided into two sets: a training set and a test set. The training set is used in network training and weights calculation, and the test set is used to validate the model. In this study, 84% of the total data were used to estimate the neural network's parameters in the training phase and 16% of the total data were used as test data to validate the networks.

4.2. Topology Selection. For selection of the best neural network model, many network topologies with different numbers of neurons in the hidden layer were tested. First a network with two neurons in a hidden layer was selected for the starting phase, and then, the network size was enlarged by adding neurons to the hidden layer. Figure 2 reveals that standard deviation of the error for networks with a low number of neurons in the hidden layer is large; it means that these networks cannot model the relationship between input and output parameters. On the other hand, networks with too many neurons in the hidden layer have the risk of overfitting, so the best topology is the networks with sufficiently low STD of error. As can be seen in Figure 2, by enlarging the model, the error of the model decreases at a fair rate, but after reaching a certain number of neurons in the hidden layer, the decreasing rate of error of the model approaches zero. After this point, the adding of a neuron to the hidden layer does not decrease the error of the model significantly, but it can cause overfitting of the model to the training data. In this work, 20 neurons in the hidden layer were considered as the optimum point, based on Figure 2.

An overview of the structural organization of the neural network used in this study can be seen in Figure 3. The optimum topology of the network includes five input variables, 20 neurons in the hidden layer, and an output variable (response) which is shown as (5, 20, 1). Each neuron (shown by the circle in the figure) in a certain layer is connected to every single neuron in the next layer. The connection between neurons is possible through links with an adjustable connection weight, which are adjusted during the training phase. In fact, weights represent the strength of the link between two neurons. A neuron receives incoming signals from each neuron of the previous layer and calculates the sum of the incoming signal's weights and then transmits it through the transfer function.

4.3. Model Validation. Figure 4 presents predicted toluene conversion versus experimental values for both training and test data. As seen, both train and test data are distributed well around y = x line with high R^2 values; 0.99 and 0.976 for training and testing data, respectively. Resulted values for R^2

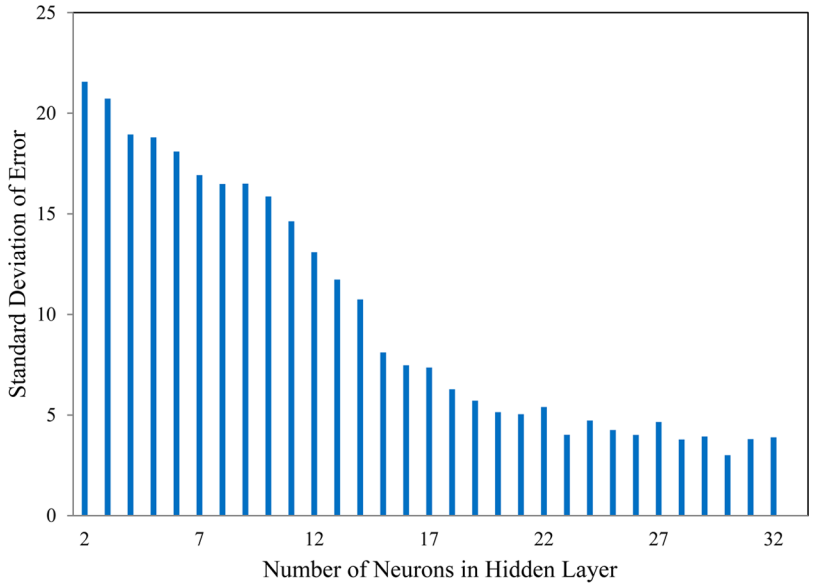

Figure 2. Standard deviation of error versus number of neurons in the hidden layer.

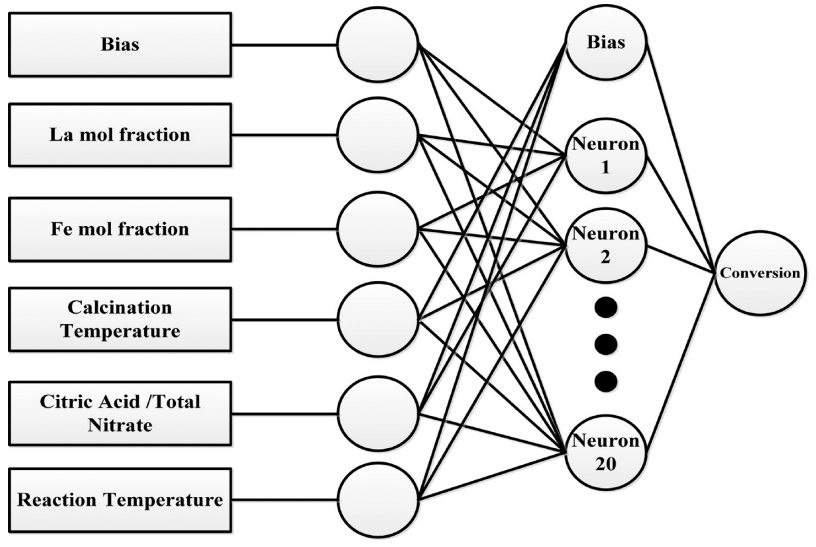

Figure 3. Neural network topology, inputs and outputs connected through a hidden layer.

indicate that the neural network model with selected topology is quite successful in predicting data. The high R^2 value for testing data is remarkable; because it shows that neural network can predict the toluene conversions for conditions that are not used during training and also it can prove that model does not overfit train data.

4.4. Effect of Design Parameters. The input significance analysis was carried out to determine the relative importance of input factors (catalyst preparation and operational variables) on toluene conversion. It was performed on the basis of the ANN model using the weights of neurons in hidden and output layers (eq 4). In fact, all input factors have a remarkable effect on toluene conversion, and none of them could be underestimated. As seen in Figure 5, reaction temperature as an operational parameter has the largest significance on catalyst performance, and among the preparation parameters, the ratio of citric acid to total nitrates is the most effective one, and calcination temperature has the lowest effect on the output parameter.

4.5. Optimum Catalysts. Normally, the neural network can be optimized by various optimizers such as a genetic algorithm to find the input variables maximizing toluene conversion. However, it was not necessary in the present case due to the presence of a full active catalyst at the minimum reaction temperature. Table 3 indicates the optimal catalysts, catalysts with 100% conversion.

4.6. Impact of Preparation Parameters on Optimum Catalyst Performance. To study the effect of preparation conditions on the performance of optimum catalysts, toluene conversion percentage (obtained model prediction) was plotted versus each preparation parameter while keeping the other parameters at their optimum values. The experimental values were shown in each plot by circle symbols. These plots for optimum catalyst no. 1, $La_{0.9}Sr_{0.1}Fe_{0.5}Co_{o.5}O_3$ (T_c = 800 °C and [mole citric acid/mol nitrate] = 0.3), are presented in Figure 6. The conversion of toluene is plotted for $La_xSr_{1-x}Fe_{0.5}Co_{o.5}O_3$ in Figure 6a for studying the effect of La and Sr molar fractions; as seen in Figure 6a, high activity for the catalyst is observed when

dx.doi.org/10.1021/co400017r | ACS Comb. Sci. 2013, 15, 609−621

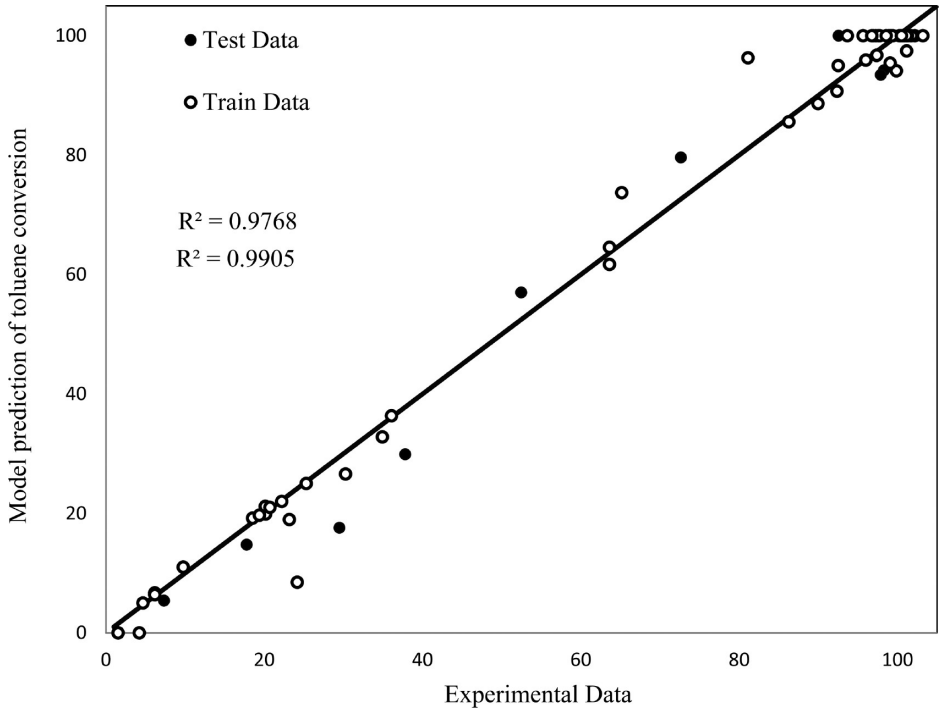

Figure 4. Model prediction versus experimental values for optimum topology (optimum topology: 5, 20, 1).

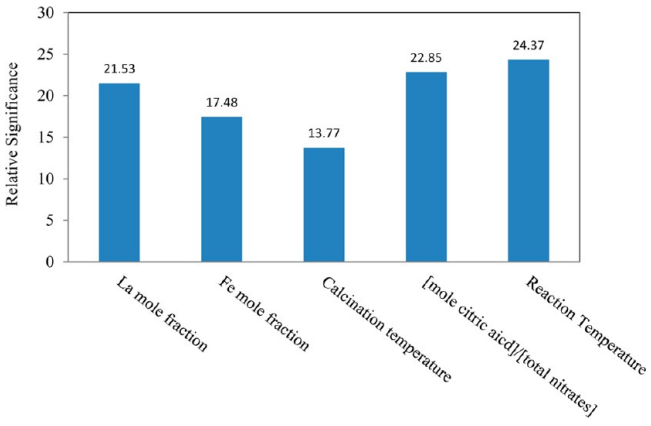

Figure 5. Relative significance of input parameters.

Table 3. Optimum Catalysts

catalyst number	catalyst	calcination temperature (°C)	[citric acid]/[total nitrate]
1	$La_{0.9}Sr_{0.1}Fe_{0.5}Co_{0.5}O_3$	800	0.3
2	$La_{0.9}Sr_{0.1}Fe_{0.5}Co_{0.5}O_3$	700	0.3
3	$La_{0.8}Sr_{0.2}Fe_{0.66}Co_{0.34}O_3$	650	0.525
4	$La_{0.9}Sr_{0.1}Fe_{0.82}Co_{0.18}O_3$	700	0.750

the mole fraction of lanthanum approaches around 0.9 (the mole fraction of strontium equals 0.1). Indeed, by introducing a bivalent strontium ion into the A site of perovskite, metal ions in the B site can get abnormal valences. These ions tend to be reduced by releasing oxygen from the lattice of perovskite (oxygen vacancies are formed) and cause an improvement in perovskite reducibility.[5] Figure 6b demonstrates the conversion of toluene versus the variations of Fe mole fraction for $La_{0.9}Sr_{0.1}Fe_yCo_{1-y}O_3$; the figure shows that maximum conversion achieves a value in the range of 0.45−0.8 mole fraction of iron. The combination of certain amounts of iron and cobalt ions at the B site improves catalyst activity, which can be attributed to the synergistic effect between iron and cobalt ions. In addition, according to model prediction, when the B-site of perovskite is occupied by cobalt ions, the activity of the catalyst is better than perovskite with iron ions in the B site. This prediction is in agreement with the other research.[6] It has been reported that regardless of elements at the A site, the catalytic activity of perovskite for oxidation is mainly determined by the type of metal at the B site.[5] The low activity of the $La_{0.9}Sr_{0.1}Fe_{0.5}Co_{0.5}O_3$ catalyst for calcination temperatures above 800 °C can be ascribed to low specific area (Figure 6c). As can be seen in Figure 6d, the highest conversion is reached at 0.2 and 0.7 [citric acid]/[total nitrate] for $La_{0.9}Sr_{0.1}Fe_{0.5}Co_{0.5}O_3$.

As mentioned before, there is a good agreement between the model prediction and the experimental data points. This is additional evidence for success of the neural network modeling.

The parameter that its variation mainly affects catalyst performance is recognized as a main and important parameter. The relative importance of input parameters for each optimum catalyst was calculated using eq 5.

$$\text{R. I}_i = \frac{\text{STD}_i}{\sum_{i=1}^{s} \text{STD}_i} \tag{5}$$

where R.I_i is the relative importance of the ith parameter, STD_i is the standard deviation of conversion while the ith parameter changes from a minimum to maximum amount and other parameters are fixed in their optimum values, and s is the number of parameters, which equals to 4 in this study. In this case, the mole fractions of lanthanum and iron are the most important parameters (Figure7). In the other words, their amounts mainly affect the activity of catalyst.

The critical value of preparation parameters was determined using eq 6. The critical parameter is defined as a parameter for which a small deviation from the optimum amount causes a significant change in catalyst performance. Identification of the

dx.doi.org/10.1021/co400017r | ACS Comb. Sci. 2013, 15, 609−621

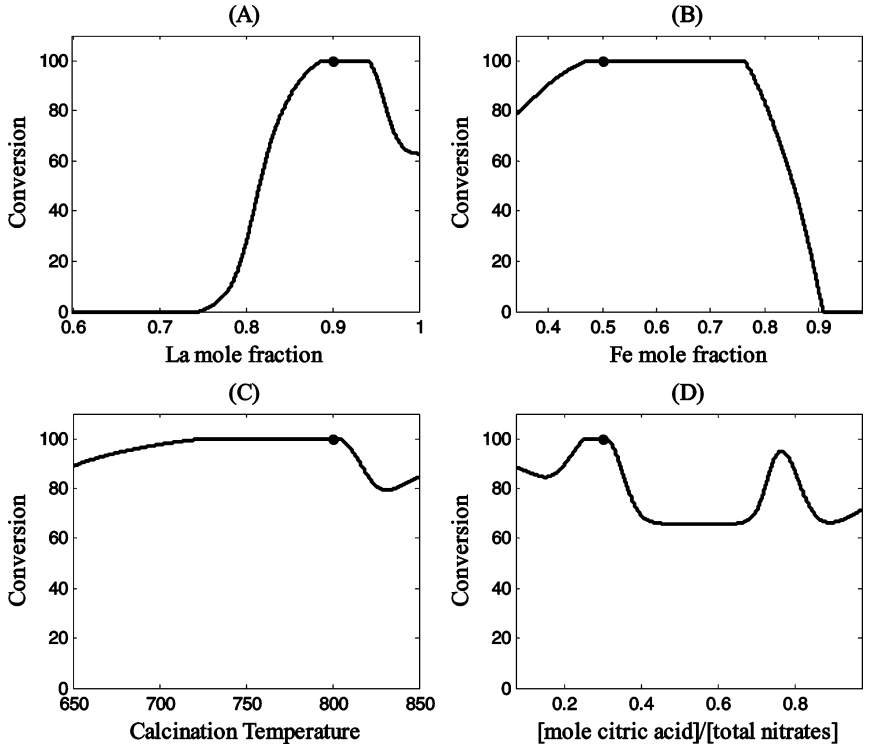

Figure 6. Conversion of $La_{0.9}Sr_{0.1}Fe_{0.5}Co_{0.5}O_3$ (T_c = 800 °C and [citric acid]/[total nitrate] = 0.3) versus preparation parameters. In each plot, other variables were fixed at their optimum values. Optimum values (experimental values) are shown with circle markers.

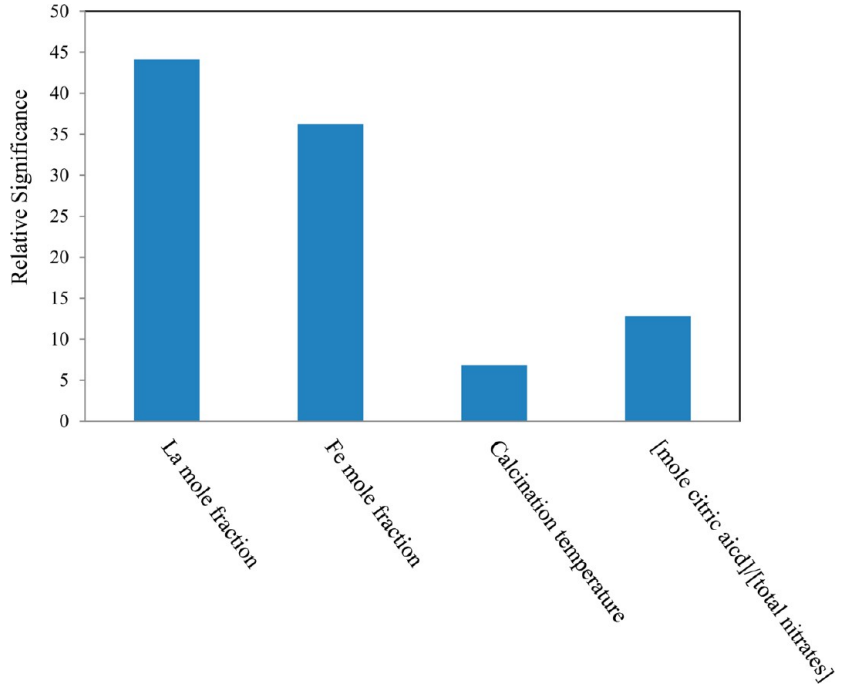

Figure 7. Relative significance of preparation parameters for $La_{0.9}Sr_{0.1}Fe_{0.5}Co_{0.5}O_3$ (T_c = 800 °C and [citric acid]/[total nitrate] = 0.3).

critical parameter is especially important for scaleup purposes and large scale production in which the critical parameters should be controlled carefully. In addition, with evaluation of criticality and catalytic behavior of samples, it is possible to change synthesis parameters to less critical values. For example, [citric acid]/[total nitrate] = 0.3 is a critical parameter in the synthesis of optimum catalyst no. 2. As seen in Figure 9d, a small deviation to lower amount significantly decreases the catalytic activity. By changing the amount of the mentioned critical parameter to a higher amount, i.e., 0.4, while the catalyst remains at high performance, the criticality of parameter decreases.

$$RC_i = \frac{STD_{i(op\pm 10\%)}}{\sum_i^4 STD_{i(op\pm 10\%)}} \quad (6)$$

dx.doi.org/10.1021/co400017r | ACS Comb. Sci. 2013, 15, 609−621

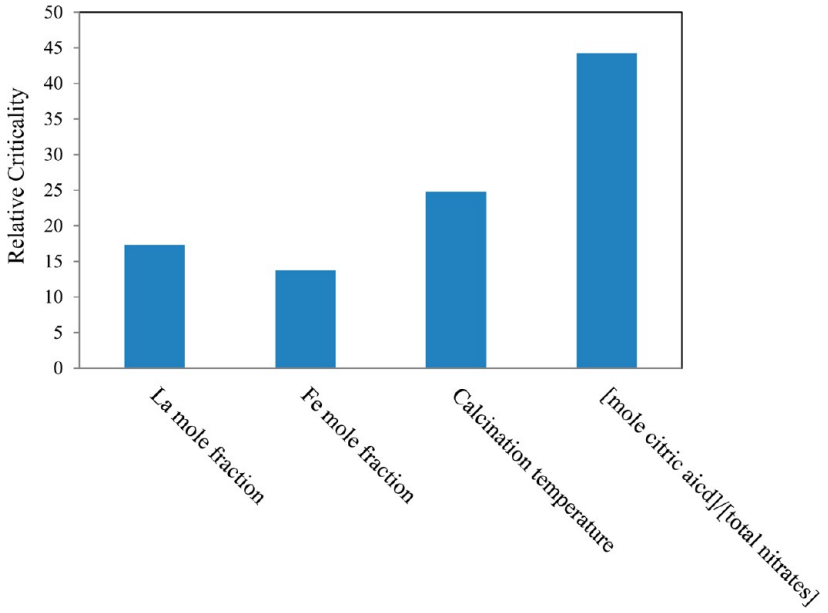

Figure 8. The critical value of preparation parameters for $La_{0.9}Sr_{0.1}Fe_{0.5}Co_{0.5}O_3$ (T_c = 800 °C and [citric acid]/[total nitrate] = 0.3).

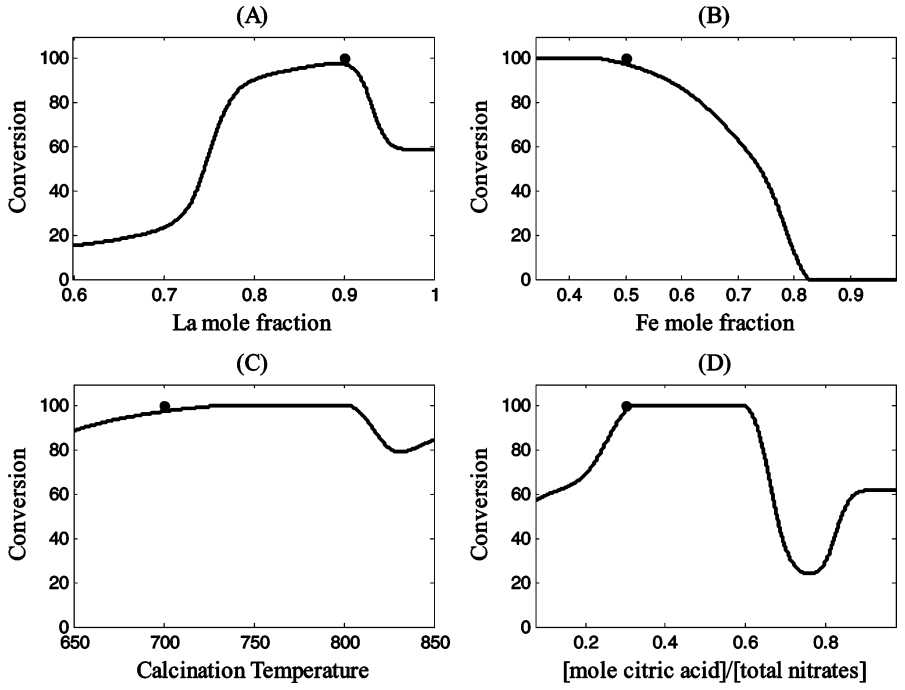

Figure 9. Conversion of $La_{0.9}Sr_{0.1}Fe_{0.5}Co_{0.5}O_3$ (T_c = 700 °C and [citric acid]/[total nitrate] = 0.3) versus preparation parameters. In each plot, other variables were fixed at their optimum values. Optimum values (experimental values) are shown with circle markers.

In eq 6, RC_i is the relative criticality of parameter i, $STD_{i(op\pm10\%)}$ is the standard deviation of conversions while the parameter i changes from optimum point −10% ($max_i - min_i$) to optimum point +10% ($max_i - min_i$). Max_i and min_i represent the maximum and minimum amounts for parameter i that were determined in the experimental design step, respectively. As seen in Figure 8, the most critical parameter for this optimum catalyst is the ratio of citric acid to total nitrate.

The effects of preparation parameters on the performance of a second optimum catalyst (Table 3) are plotted in Figure 9. The effect of lanthanum mole fraction on the performance of $La_xSr_{1-x}Fe_{0.5}Co_{0.5}O_3$ is plotted in Figure 9a. Figure 9a indicates that toluene conversion has been improved significantly by the Sr substitution. This catalyst shows high catalytic activity when the mole fraction of iron is lower than 0.5 in $La_{0.9}Sr_{0.1}Fe_yCo_{1-y}O_3$ (Figure 9b). Some intermediate levels of molar citric acid to molar nitrate (0.3−0.6) seem to be more suitable for this catalyst with the $La_{0.9}Sr_{0.1}Fe_{0.5}Co_{0.5}O_3$ formula (Figure 9d). According to Figure 9c, calcination at temperatures above 800 °C can promote sintering and subsequently decrease the activity of the catalyst.

Similar results can be seen for the two other optimum catalysts; Sr substitution improved the catalyst activity in toluene combustion (Figures 10a and 11a). Figures 10a and 11a show the catalytic activity of $La_xSr_{1-x}Fe_{0.66}Co_{0.34}O_3$ and $La_xSr_{1-x}Fe_{0.82}Co_{0.18}O_3$ for toluene combustion, respectively.

dx.doi.org/10.1021/co400017r | ACS Comb. Sci. 2013, 15, 609−621

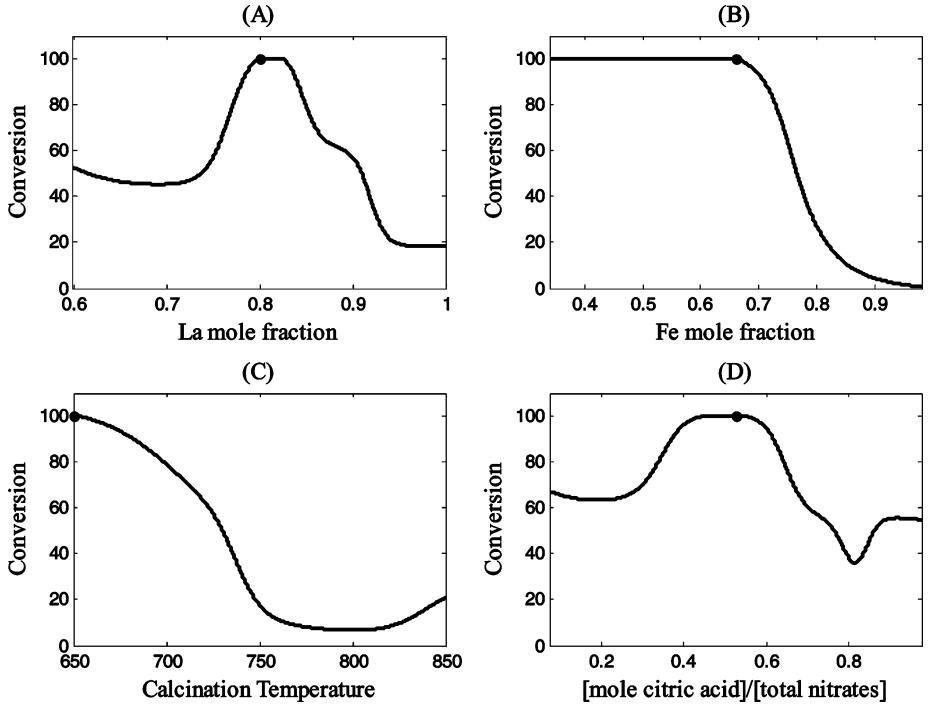

Figure 10. Conversion of $La_{0.8}Sr_{0.2}Fe_{0.66}Co_{0.34}O_3$ (T_c = 650 °C and [citric acid]/[total nitrate] = 0.525) versus preparation parameters. In each plot, other variables were fixed at their optimum values. Optimum values (experimental values) are shown with circle markers.

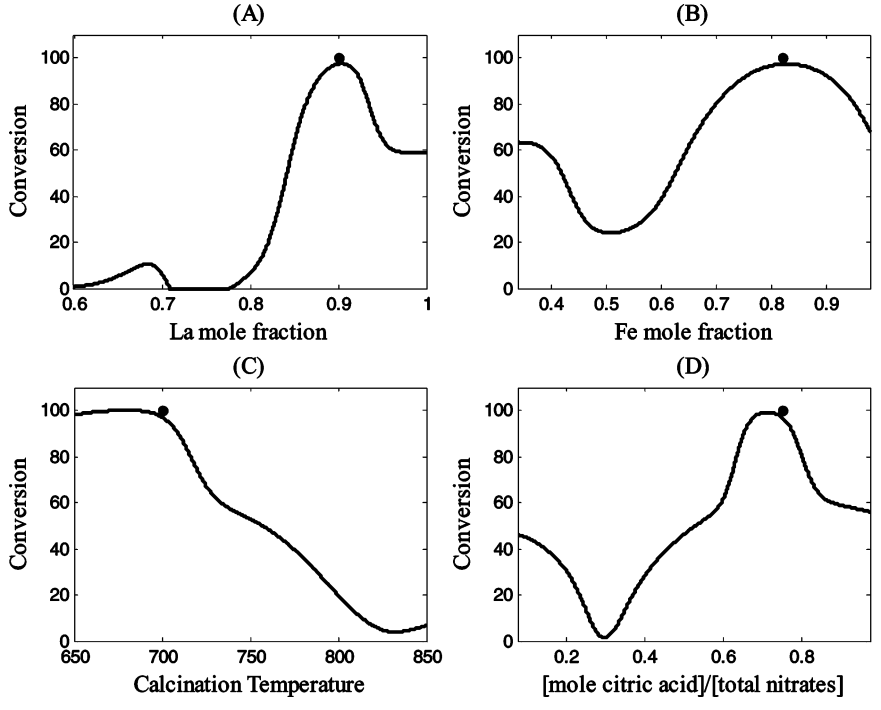

Figure 11. Conversion of $La_{0.9}Sr_{0.1}Fe_{0.82}Co_{0.18}O_3$ (T_c = 700 °C and [citric acid]/[total nitrate] = 0.750) versus preparation parameters. In each plot, other variables were fixed at their optimum values. Optimum values (experimental values) are shown with circle markers.

Due to the synergistic effect between iron and cobalt cations, the coexistence of cobalt and iron in the perovskite structure enhanced the catalyst performance (Figures 10b and 11b). In addition, because of sintering at high temperatures, the catalyst activity decreased as the calcination temperature increased (Figures 10c and 11c). The molar ratio of citric acid to total nitrates has a volcano shaped effect on catalyst performance (Figures 10d and 11d).

Figure 12 shows the relative criticality of preparation parameters calculated by using eq 6 for the other optimum catalysts. The critical parameter for each optimum catalyst has been determined in Table 4.

4.7. Characterization. Among the 31 catalysts suggested by CCD, the structure of five catalysts with different preparation conditions was investigated using the X-ray diffraction method. A comparison of XRD patterns with

dx.doi.org/10.1021/co400017r | ACS Comb. Sci. 2013, 15, 609−621

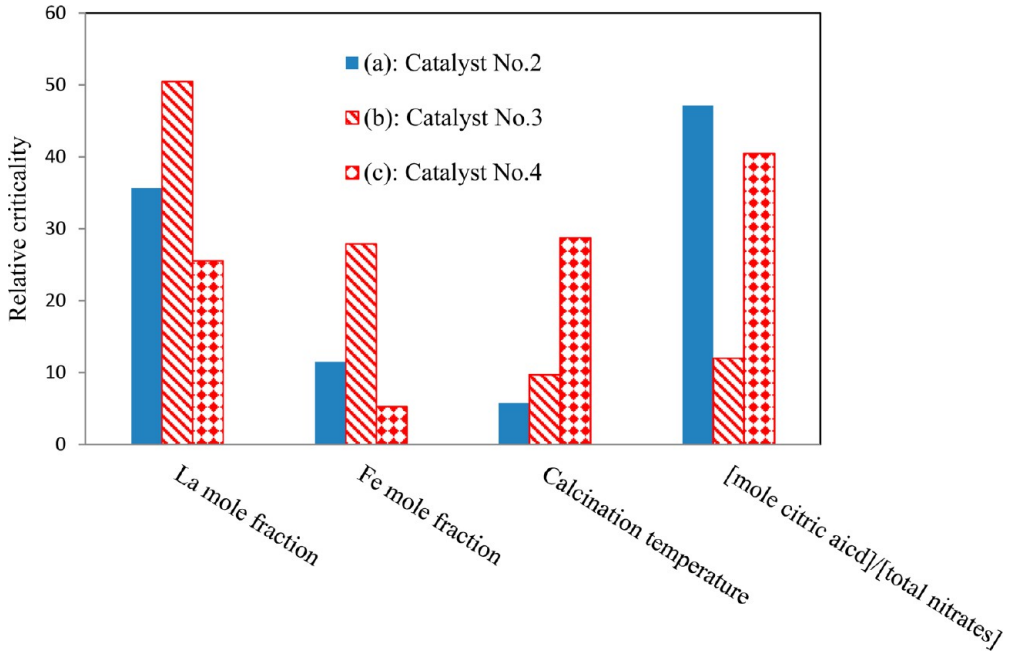

Figure 12. Critical value of $La_{0.9}Sr_{0.1}Fe_{0.5}Co_{0.5}O_3$ (T_c = 700 °C and [citric acid]/[total nitrate] = 0.3) (a), $La_{0.8}Sr_{0.2}Fe_{0.66}Co_{0.34}O_3$ (T_c = 650 °C and [citric acid]/[total nitrate] = 0.525) (b), $La_{0.9}Sr_{0.1}Fe_{0.82}Co_{0.18}O_3$ (T_c = 700 °C and [citric acid]/[total nitrate] = 0.750) (c).

Table 4. Critical Parameter in Optimum Catalysts

catalyst number	catalyst	calcination temperature (°C)	[citric acid]/[total nitrate]	critical parameter
1	$La_{0.9}Sr_{0.1}Fe_{0.5}Co_{0.5}O_3$	800	0.3	[citric acid]/[total nitrate]
2	$La_{0.9}Sr_{0.1}Fe_{0.5}Co_{0.5}O_3$	700	0.3	[citric acid]/[total nitrate]
3	$La_{0.8}Sr_{0.2}Fe_{0.66}Co_{0.34}O_3$	650	0.525	mole fraction of lanthanum
4	$La_{0.9}Sr_{0.1}Fe_{0.82}Co_{0.18}O_3$	700	0.75	[citric acid]/[total nitrate]

JCPDS 48-0123 and JCPDS 37-14983 charts indicated that catalysts were single-phase perovskite oxides. The average crystal sizes of the perovskites were calculated using the sharpest characteristic peak (2θ of 32.9°) through the Scherer equation, and the results are presented in Table 5.

Table 5. Crystal Diameter of Perovskites

catalyst number	catalyst	calcination temperature (°C)	[citric acid]/[total nitrate]	crystal diameter (nm)
1	$La_{0.8}Sr_{0.2}Fe_{0.66}Co_{0.34}O_3$	750	0.525	18
2	$La_{0.8}Sr_{0.2}Fe_{0.66}$ $Co_{0.34}O_3$	750	0.975	19
3	$La_1Fe_{0.66}Co_{0.34}O_3$	750	0.525	22
4	$La_{0.8}Sr_{0.2}Fe_{0.34}Co_{0.66}O_3$	750	0.525	16
5	$La_{0.8}Sr_{0.2}Fe_{0.66}$ $Co_{0.34}O_3$	650	0.525	12

The size and morphology of perovskite catalysts were investigated by scanning electron microscopy (SEM) as shown in Figure 13. It is observed that the morphologies of particles are spherical, and the particles of the catalysts are within the nanoscale (≤100 nm).

The H_2-TPR studies were carried out to investigate the effect of substitution amount of the cobalt ion in the B site and partial substitution of Sr^{2+} in the A site on the reducibility of catalysts. Also, the H_2-TPR profiles were used to interpret the observed catalytic behavior and as a confirmation for model prediction.

Regarding the H_2-TPR profile of $LaFe_{0.66}Co_{0.34}O_3$ (Figure 14a), one peak centered on 480 °C and a shoulder on the low temperature side of the mentioned peak are observed relating to the reduction of Co^{3+} to Co^{2+} and Fe^{4+} to Fe^{3+}, respectively. In the TPR profile of $La_{0.8}Sr_{0.2}Fe_{0.66}Co_{0.34}O_3$, the first peak (329 °C) overlaps with the second peak (383 °C), and they are attributed to the reduction of Fe^{4+} to Fe^{3+} and Co^{3+} to Co^{2+}, respectively (Figure 14b). Apparently, with the doping of strontium, the intensity of the Fe^{4+} reduction peak increased, indicating the higher content of Fe^{4+}, and the reduction peak of Co^{3+} shifted toward lower temperature; i.e., the addition of strontium at the A site of the $LaFe_{0.66}Co_{0.34}O_3$ increased the reducibility of the catalyst. The obtained result is in agreement with experimental data (Supporting Information). In addition, H_2-TPR profiles confirmed the prediction of the model about the presence of strontium in a perovskite structure.

As seen from the H_2-TPR profile of $La_{0.8}Sr_{0.2}Fe_{0.34}Co_{0.66}O_3$ (Figure 14c), the first peak overlaps with a second peak, and their highest temperatures are 346 and 358 °C. The mentioned peaks are assigned to the Co^{3+} to Co^{2+} and Fe^{4+} to Fe^{3+} reductions, respectively. The reduction temperatures of Fe^{4+} and Co^{3+} in the $La_{0.8}Sr_{0.2}Fe_{0.34}Co_{0.66}O_3$ profile did not shift compared to those in $La_{0.8}Sr_{0.2}Fe_{0.66}Co_{0.34}O_3$ profile, just the intensity of both peaks increased, which is attributed to an increase in the number of Fe^{4+} and Co^{3+}. It shows that the reduction ability of the catalyst increases as the amount of cobalt ions in the B site increases.

Specific surface areas of the perovskites are presented in Table 6. As seen, the specific surface areas are in the range of 5−11 $m^2\ g^{-1}$. The change in specific surface area with calcination temperature is an important parameter that affects the catalytic activity. As seen in Table 6, catalyst number four

dx.doi.org/10.1021/co400017r | ACS Comb. Sci. 2013, 15, 609−621

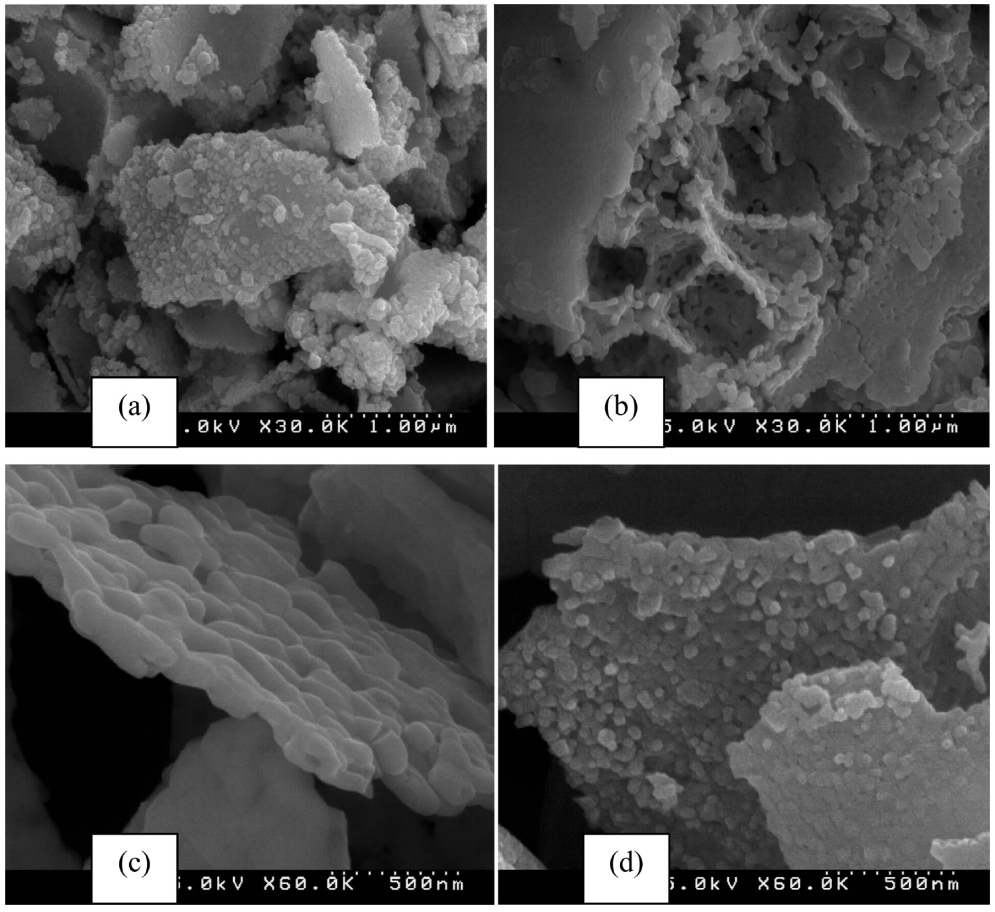

Figure 13. SEM image of $La_{0.8}Sr_{0.2}Fe_{0.66}Co_{0.34}O_3$ (T_c = 750 °C and [citric acid]/[total nitrate] = 0.525) (a), $La_{0.8}Sr_{0.2}Fe_{0.66}Co_{0.34}O_3$ (T_c = 750 °C and [citric acid]/[total nitrate] = 0.975) (b), $LaFe_{0.66}Co_{0.34}O_3$ (T_c = 750 °C and [citric acid]/[total nitrate] = 0.525) (c), $La_{0.8}Sr_{0.2}Fe_{0.34}Co_{0.66}O_3$ (T_c = 750 °C and [citric acid]/[total nitrate] = 0.525) (d).

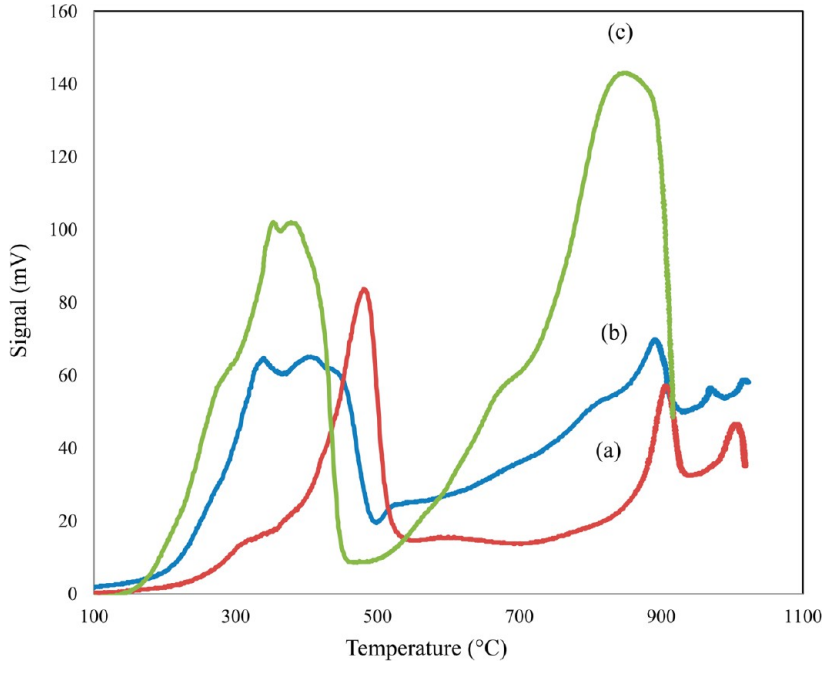

Figure 14. TPR curves of $LaFe_{0.66}Co_{0.34}O_3$ (T_c = 750 °C and [citric acid]/[total nitrate] = 0.525) (a), $La_{0.8}Sr_{0.2}Fe_{0.66}Co_{0.34}O_3$ (T_c = 750 °C and [citric acid]/[total nitrate] = 0.525) (b), $La_{0.8}Sr_{0.2}Fe_{0.34}Co_{0.66}O_3$ (T_c = 750 °C and [citric acid]/[total nitrate] = 0.525) (c).

dx.doi.org/10.1021/co400017r | ACS Comb. Sci. 2013, 15, 609−621

Table 6. Specific Surface Area of Perovskites

catalyst number	catalyst	calcination temperature (°C)	[citric acid]/[total nitrate]	specific surface area ($m^2\ g^{-1}$)
1	$La_{0.8}Sr_{0.2}Fe_{0.66}Co_{0.34}O_3$	750	0.525	5.26
2	$LaFe_{0.66}Co_{0.34}O_3$	750	0.525	8.15
3	$La_{0.8}Sr_{0.2}Fe_{0.34}Co_{0.66}O_3$	750	0.525	8.78
4	$La_{0.8}\ Sr_{0.2}Fe_{0.66}\ Co_{0.34}O_3$	650	0.525	10.62

with a low calcination temperature shows high catalytic activity due to high surface area in comparison with catalyst number one. The specific surface area decreased by introducing Sr^{2+} to the perovskite structure, while the catalytic activity increased. This result shows that there is not any direct relationship between specific surface area and catalytic activity of perovskite. Previously our group reported a similar result in the catalytic combustion of toluene over perovskite catalysts.[18,25] Data indicate that specific surface area and catalytic activity of perovskite have been increased by increasing the molar ratio of cobalt in B sites (comparison catalysts number one and three). Overall, considering both the catalytic activities of perovskites and their specific surface area shows that the composition of perovskite has more influence on the catalytic activity than specific surface area.

5. CONCLUSION

$La_xSr_{1-x}Fe_yCo_{1-y}O_3$ perovskite, prepared with the sol−gel method, was used as a novel catalyst for catalytic oxidation of toluene. For the first time, ANN was applied for modeling the composition−activity relationship in perovskite catalysts for the toluene combustion process. A three-layer perceptron neural network was used for modeling and expressing the relationship between catalytic performance and catalyst design parameters. Due to the presence of full active catalysts, an optimizer algorithm such as a genetic algorithm was not used. The optimum catalysts exhibiting 100% conversion for toluene were $La_{0.9}Sr_{0.1}Fe_{0.5}Co_{0.5}O_3$ (Tc = 700 and 800 °C and [citric acid/nitrate] = 0.3), $La_{0.9}Sr_{0.1}Fe_{0.82}Co_{0.18}O_3$ (Tc = 700 °C, [citric acid/total nitrate] = 0.750), and $La_{0.8}Sr_{0.2}Fe_{0.66}Co_{0.34}O_3$ (Tc = 650 °C, [citric acid/total nitrate] = 0.525). In addition, parameter space evaluation of perovskite synthesis (as pioneer insight) is carried out by using the obtained ANN model. Gained results are in agreement with the other experimental reports. Regarding the model, all of the preparation parameters have an important effect on catalyst performance.

■ ASSOCIATED CONTENT

Supporting Information

Data utilized for modeling of composition−activity relationship is available in this file as a table. This information is available free of charge via the Internet at http://pubs.acs.org.

■ AUTHOR INFORMATION

Corresponding Author

*Tel.: 00984113393163. Fax: 00984113340191. E-mail: niaei@yahoo.com.

Notes

The authors declare no competing financial interest.

■ ACKNOWLEDGMENTS

The authors are thankful to those who contributed to enhancing this project, especially Iranian Nanotechnology Initiative Council for financial supports

■ REFERENCES

(1) Demeestere, K.; Dewulf, J.; De Witte, B.; Van Langenhove, H. Sample preparation for the analysis of volatile organic compounds in air and water matrices. *J. Chromatogr., A* **2007**, *1153*, 130−144.
(2) Calvert, J. G. Chemistry for the 21st Century. *The Chemistry of the Atmosphere: Its Impact on Global Change*; Blackwell Scientific Publications: Oxford, 1994.
(3) Forst, L.; Conroy, L. M. *Odors and VOC Control Handbook*; Rafson, H. J., Eds.; McGraw-Hill: New York, 1998.
(4) Chang, C. C.; Weng, H. S. Deep Oxidation of Toluene on Perovskite Catalyst. *Ind. Eng. Chem. Res.* **1993**, *32*, 2930−2933.
(5) Tanaka, H.; Misono, M. Advances in designing perovskite catalysts. *Curr. Opin. Solid State Mater. Sci.* **2001**, *5*, 381−387.
(6) Peña, M. A.; Fierro, J. L. G. Chemical Structures and Performance of Perovskite Oxides. *Chem. Rev.* **2001**, *101*, 1981−2017.
(7) Günay, M. E.; Yıldırım, R. Neural network aided design of Pt-Co-Ce/Al_2O_3 catalyst for selective CO oxidation in hydrogen-rich streams. *Chem. Eng. J.* **2008**, *140*, 324−331.
(8) Huang, K.; Zhan, X. L.; Chen, F. Q.; Lü, D. W. Catalyst design for methane oxidative coupling by using artificial neural network andhybridgenetic algorithm. *Chem. Eng. Sci.* **2003**, *58*, 81−87.
(9) Liu, Y.; Liu, Y.; Liu, D.; Cao, T.; Han, S.; Xu, G. Design of CO_2 hydrogenation catalyst by an artificial neural network. *Comput. Chem. Eng.* **2001**, *25*, 1711−1714.
(10) Maier, W. F.; Stowe, K.; Sieg, S. Combinatorial and high-throughput materials science. *Angew. Chem. Int. Ed.* **2007**, *46*, 6016−6067.
(11) Hou, Z. Y.; Dai, Q. L.; Wu, X. Q.; Chen, G. T. Artificial neural network of catalyst for propane ammoxidation. *Appl. Catal., A* **1997**, *161*, 183−190.
(12) Huang, K.; Chen, F.; Lü, D. Artificial neural network-aided design of a multi-component catalyst for methane oxidative coupling. *Appl. Catal., A* **2001**, *219*, 61−68.
(13) Serra, J. M.; Corma, A.; Argente, E.; Valero, S.; Botti, V. Neural networks for modelling of kinetic reaction data applicable to catalyst scale up and process control and optimization in the frame of combinatorial catalysis. *Appl. Catal., A* **2003**, *254*, 133−145.
(14) Baumes, L.; Farrusseng, D.; Lengliz, M.; Mirodatos, C. Using Artificial Neural Networks to boost high-throughput discovery in heterogeneous catalysis. *QSAR Comb. Sci.* **2004**, *23*, 767−778.
(15) Izadkhah, B.; Nabavi, S. R.; Niaei, A.; Salari, D.; Mahmuodi Badiki, T.; Çaylak, N. Design and optimization of Bi-metallic Ag-ZSM5 catalysts for catalytic oxidation of volatile organic compounds. *J. Ind. Eng. Chem.* **2012**, *18*, 2083−2091.
(16) Niaei, A.; MahmuodiBadiki, T.; Nabavi, S. R.; Salari, D.; Izadkhah, B.; Çaylak, N. Neuro-genetic aided design of modified H-ZSM-5 catalyst for catalytic conversionof methanol to gasoline range hydrocarbons. *J. Taiwan Inst. Chem. Eng.* **2012**, *44*, 247−256.
(17) Huang, H.; Liu, Y.; Tang, W.; Chen, Y. Catalytic activity of nanometer $La_{1-x}Sr_xCoO_3$ (x=0, 0.2) perovskites towards VOCs combustion. *Catal. Commun.* **2008**, *9*, 55−59.
(18) Hosseini, S. A.; Sadeghi, M. T.; Alemi, A.; Niaei, A.; Salari, D.; Kafi-Ahmadi, L. Synthesis, Characterization and Performance of $LaZn_xFe_{1-x}O_3$ Perovskite Nanocatalysts for toluene combustion. *Chin. J. Catal.* **2010**, *31*, 747−750.
(19) Ziegel, E. R. Experimental design for combinatorial and high throughput materials development. *Technometrics* **2003**, *45*, 365−365.
(20) Holena, M.; Baerns, M. Feedforward neural networks in catalysis-A tool for the approximation of the dependency of yield on catalyst composition, and for knowledge extraction. *Catal. Today* **2003**, *81*, 485−494.
(21) Sasaki, M.; Hamada, H.; Kintaichi, Y.; Ito, T. Application of a neural network to the analysis of catalytic reactions Analysis of NO

decomposition over Cu/ZSM-5 zeolite. *Appl. Catal., A* **1995**, *132*, 261−270.
(22) Ahari, J. S.; Sadeghi, M. T.; Pashne, S. Z. Optimization of OCM reaction conditions over Na−W−Mn/SiO2 catalyst at elevated pressure. *J. Taiwan Inst. Chem. Eng.* **2011**, *42*, 751−759.
(23) Hormik, K.; Stinchcombe, H.; White, H. Multilayer Feedforward Networks are Universal Approximators. *Neural Networks* **1989**, *2*, 359−366.
(24) Garson, G. D. Interpreting neural network connection weights. *Artif. Intell. Expert Syst.* **1991**, *6*, 47−51.
(25) Hosseini, S. A.; Salari, D.; Niaei, A.; Arefi Oskoui, S. Physical-chemical property and activity evaluation of $LaB_{0.5}Co_{0.5}O_3$ (B= Cr, Mn, Cu) and $LaMn_xCo_{1-x}O_3$ (x= 0.1, 0.25, 0.5) nano perovskites in VOC combustion. *J. Ind. Eng. Chem.* **2013**, DOI: 10.1016/j.jiec.2013.02.034..